Single production of excited electrons at future e^+e^-, ep and pp colliders

O. Çakır* and A. Yılmaz
Ankara University, Faculty of Sciences, Department of Physics, 06100, Tandogan, Ankara, Turkey

S. Sultansoy†
Gazi University, Faculty of Arts and Sciences, Department of Physics, 06500, Teknikokullar, Ankara, Turkey and Azerbaijan Academy of Sciences, Institute of Physics, H. Cavid Ave. 33, Baku, Azerbaijan.

We analyzed the potential of the LC with $\sqrt{s} = 0.5$ TeV, LC⊗LHC based ep collider with $\sqrt{s} = 3.74$ TeV and the LHC with $\sqrt{s} = 14$ TeV to search for excited electrons through transition magnetic type couplings with gauge bosons. The $e^\star \to e\gamma$ signal and corresponding backgrounds are studied in detail.

arXiv:hep-ph/0403307v5 20 Jul 2004

I. INTRODUCTION

Three types of colliders related to the energy frontiers in particle physics research seem to be promising in the next decade. Namely, they are Large Hadron Collider (LHC) with the center of mass energy $\sqrt{s} = 14$ TeV and luminosity $L = 10^{34} - 10^{35}\text{cm}^{-2}\text{s}^{-1}$, linear e^+e^- collider (LC) with $\sqrt{s} = 0.5$ TeV and $L = 10^{34} - 10^{35}\text{cm}^{-2}\text{s}^{-1}$, and linac-ring type ep collider (LC⊗LHC) with $\sqrt{s} = 3.74$ TeV and $L = 10^{31} - 10^{32}\text{cm}^{-2}\text{s}^{-1}$ (see [1] and references therein). Even though the last one has a lower luminosity it can provide better conditions for investigations of a lot of phenomena comparing to LC due to the essentially higher center of mass energy and LHC due to more clear environment. For this reason, different phenomena (compositeness, SUSY, etc.) should be analyzed taking into account all three types of colliders.

The fundamental questions left open by the Standard Model (SM), such as the number of fermion families, the fermion masses and the mixings, are addressed by composite models [2]. In the framework of composite models of quarks and leptons, constituents of known fermions interact by means of new interactions. A non-trivial substructure of known fermions leads to a rich spectrum of excited states [3]. Phenomenologically, an excited lepton is defined to be a heavy lepton which shares leptonic quantum numbers with one of the existing leptons. Charged ($e^\star, \mu^\star$ and $\tau^\star$) and neutral ($\nu_e^\star, \nu_\mu^\star$ and $\nu_\tau^\star$) excited leptons are predicted by composite models where leptons and quarks have substructure.

Current limits on the mass of the excited electron are [4]: $m_\star > 100$ GeV from LEP (pair production) assuming $f = f'$ [5], $m_\star > 223$ GeV from HERA (single production) assuming $f = f' = \Lambda/m_\star$ [6] and $m_\star > 310$ GeV from LEP (indirect) assuming $\lambda_\gamma = 1$ [7].

On the theoretical side, the production of excited leptons was studied at LEP and HERA energies [8] and at hadron colliders [9] by taking into account only the signal. The LEP and HERA bounds on excited lepton masses are low enough when compared to the expected scale for the compositeness. This motivates us to reanalyze the excited lepton production at the future colliders. In this paper, we go beyond by studying the signal as well as the background (with the interference between them) at the similar experimental conditions and compare the potential of each type of colliders to search for the single production of excited electrons.

The interaction between an excited lepton, gauge bosons and the SM leptons is described by $SU(2) \times U(1)$ invariant lagrangian [8, 9, 10]

$$L = \frac{1}{2\Lambda} \bar{l_R^\star} \sigma^{\mu\nu} \left[f g \frac{\overrightarrow{\tau}}{2} \cdot \overrightarrow{W}_{\mu\nu} + f^{'} g^{'} \frac{Y}{2} B_{\mu\nu} \right] l_L + h.c. \tag{1}$$

where Λ is the scale of the new physics responsible for the existence of excited leptons; $W_{\mu\nu}$ and $B_{\mu\nu}$ are the field strength tensors; $\overrightarrow{\tau}$ denotes the Pauli matrices, $Y = -1/2$ is the hypercharge; g and $g^{'}$ are the SM gauge couplings of SU(2) and U(1), respectively; the constants f and $f^{'}$ are the scaling factors for the corresponding gauge couplings. In these expressions, $\sigma^{\mu\nu} = i(\gamma^\mu\gamma^\nu - \gamma^\nu\gamma^\mu)/2$ where γ^μ are the Dirac matrices.

*Electronic address: ocakir@science.ankara.edu.tr
†Electronic address: saleh@gazi.edu.tr

For an excited electron, three decay modes are possible: radiative decays $e^\star \to e\gamma$, charged current decays $e^\star \to \nu W$, neutral currents decays $e^\star \to eZ$. Neglecting ordinary lepton masses the decay widths are obtained as [9, 10]

$$\Gamma(e^\star \to lV) = \frac{\alpha m_\star^3}{4\Lambda^2} f_V^2 \left(1 - \frac{m_V^2}{m_\star^2}\right)^2 \left(1 + \frac{m_V^2}{2m_\star^2}\right) \tag{2}$$

where $f_\gamma = -(f + f^{'})/2$, $f_W = f/(\sqrt{2} sin\theta_W)$ and $f_Z = (-f cos^2\theta_W + f^{'} sin^2\theta_W)/2$. The total decay width Γ of the excited electron and the relative branching ratios (BR) into ordinary leptons and gauge bosons γ, Z, W are given in Fig. 1. For a comparison, in Fig. 1(a) we show the total decay widths of excited electron for $\Lambda = m^\star$and $\Lambda = 1$ TeV, which are commonly used for the new physics scale. For large values of the excited electron mass, the branching ratio for the individual decay channels reaches to the constant values 60% for the W-channel, 12% for the Z-channel and 28% for the photon channel. The branching ratios in these different modes depend on the relative values of f and $f^{'}$. For $f = f^{'}$, the radiative decay is allowed for excited electron whereas it is forbidden for excited neutrino.

II. SINGLE PRODUCTION OF EXCITED ELECTRONS

We analyze the potentials of the LC, LC⊗LHC and LHC machines to search for excited electrons (or positrons) via the single production reactions

$$e^+e^- \to e^{\pm\star}e^\mp \tag{3}$$

$$e^-p \to e^{-\star}q(\bar{q})X \tag{4}$$

$$pp \to e^{\pm\star}e^\mp X \qquad \text{and} \qquad pp \to e^{-(+)\star}(\overline{\nu})\nu X \tag{5}$$

with subsequent decay of excited electron (or positron) into photon and an electron (or positron). Therefore, we deal with the process $e^+e^- \to \gamma e^\pm e^\mp$, and subprocesses $e^-q(\bar{q}) \to \gamma e^- q(\bar{q})$, $q\bar{q} \to \gamma e^\pm e^\mp$ and $q\bar{q}' \to \gamma e^{-(+)}(\bar{\nu})\nu$. The signal and background were simulated at the parton level by using the program CompHEP 4.2 [11] (the interference terms between signal and background processes are included). In our calculations we used the parton distribution functions library CTEQ6L [12] with the factorization scale $Q^2 = \hat{s}$.

For a comparison of different colliders, the signal cross sections for the processes given above are presented in Fig. 2 assuming the scale $\Lambda = m_*$ and the coupling parameters $f = f^{'} = 1$.

A. e^-e^+ Collider

High energy electron-positron collisions constitute an excellent environment for the search for excited leptons. We examine the single production of excited electrons ($e^\star$) at future e^-e^+ colliders with $\sqrt{s} = 500$ GeV, through the process $e^-e^+ \to e^{\pm\star}e^\mp \to e^\pm e^\mp\gamma$. The Feynman diagram for the process $e^-e^+ \to e^{-\star}e^+$ is shown in Fig. 3.

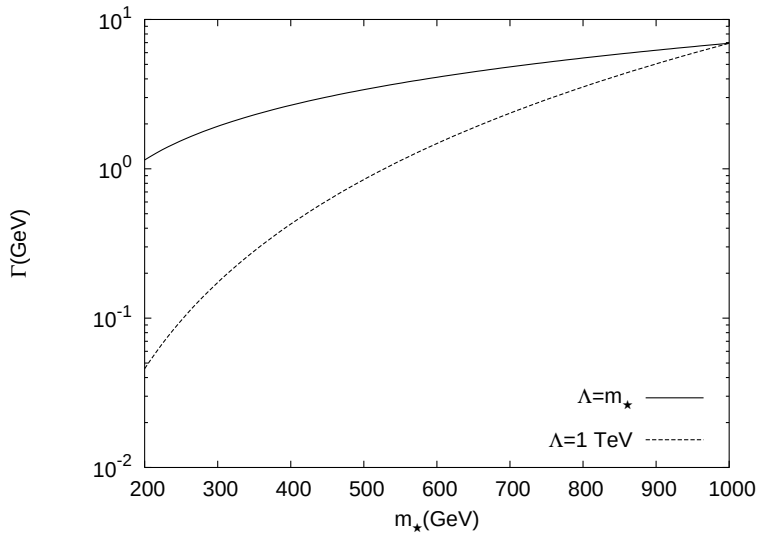
We applied to this process the following acceptance cuts

$$p_T^{e,\gamma} > 20 \text{ GeV} \tag{6}$$

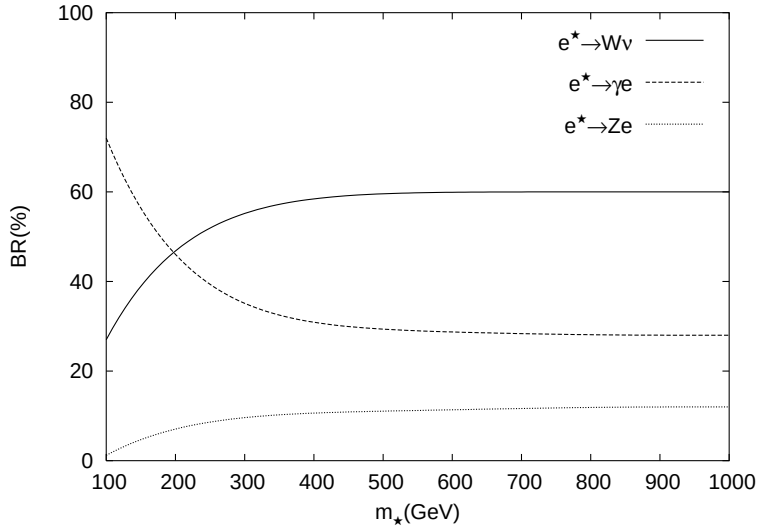
$$|\eta_{e^\pm,\gamma}| < 2.5 \tag{7}$$

$$\Delta R_{(e^+e^-),(e^\pm\gamma)} > 0.4 \tag{8}$$

where p_T is the transverse momentum of the visible particle. η stands for the pseudo-rapidity of the visible particles and $\Delta R = \sqrt{\Delta\eta^2 + \Delta\phi^2}$ is the separation between two of them. After applying these cuts, the SM background



(a)



(b)

Figure 1: (a) The total decay width Γ in GeV of excited electron for the scale $\Lambda = 1$ TeV and $\Lambda = m_\star$ with the couplings $f = f' = 1$, and (b) the branching ratios BR (%) depending on the mass of excited electron for $f = f' = 1$.

cross section is found to be $\sigma = 1.93$ pb. The $e\gamma$ decay products of excited electron can be easily identified since they typically have large transverse momentum of about $m_*/2$. Fig. 4 shows the invariant mass $m_{e\gamma}$ distribution in the reaction $e^+e^- \to e^+e^-\gamma$ for the SM and with the inclusion of an excited electron with masses $m_\star = 200$ GeV, $m_\star = 300$ GeV, $m_\star = 400$ GeV and parameter$f = f^{'} = 1$.

A natural way to extract the excited electron signal, and at the same time suppress the SM backgrounds, is to impose a cut on the $e\gamma$ invariant mass. Therefore, we introduced the cut

$$|m_{e^\pm\gamma} - m_\star| < 25 \text{ GeV} \tag{9}$$

for considered excited electron mass range. In Table I, we have presented the signal (for $f = f^{'} = 1$) and background cross sections in $e\gamma$ invariant mass bins since the signal is concentrated in a small region proportional to the invariant mass resolution. In order to examine the potential of the collider to search for the excited electron, we defined the

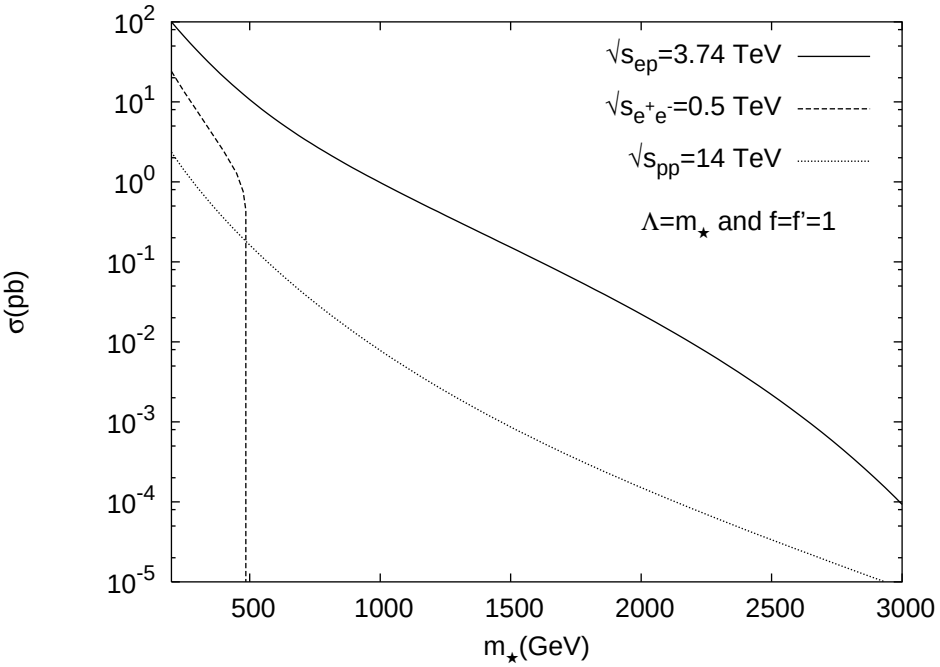


Figure 2: The total cross sections for the single production of excited electron at e^-e^+ collider with $\sqrt{s} = 0.5$ TeV, ep collider with $\sqrt{s} = 3.74$ TeV and pp collider with $\sqrt{s} = 14$ TeV.

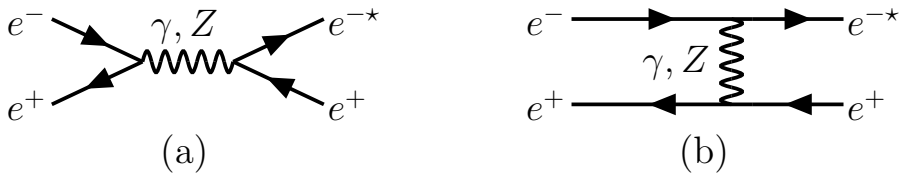


Figure 3: Excited electron production at e^-e^+ colliders through the (a) $s-$channel and (b) $t-$ channel exchange diagrams.

statistical significance SS of the signal

$$SS = \frac{|\sigma_{S+B} - \sigma_B|}{\sqrt{\sigma_B}} \sqrt{L_{int}} \tag{10}$$

where L_{int} is the integrated luminosity of the collider. The values of SS evaluated at each excited electron mass points are shown in the last column of Table I. As seen from the Table I the calculated SS values are higher than 5 up to the center of mass energy of the LC. Single production of excited electrons is dominated by the t-channel γ exchange contribution which makes its detection feasible up to masses next to the e^+e^- collider center of mass energy even with fairly small magnetic transition couplings to electrons. For various coupling parameters $f(= f^{'})$, we give the SS values in Fig. 5. Concerning the criteria above (SS>5), even for smaller coupling as $f = f' = 0.1$ excited electrons with masses up to 375 GeV can be probed at the LC.

B. ep Collider

The magnetic transition couplings of excited electron to the electron allows single production of $e^\star$ through t-channel γ and Z exchange. The Feynman diagrams for the subprocess $e^-q \to e^{-\star}q$ and $e^-\overline{q} \to e^{-\star}\overline{q}$ are shown in Fig. 6. After the acceptance cuts the total SM background cross section is obtained as $\sigma_B = 4.29$ pb. Fig. 7 shows the invariant mass $m_{e\gamma}$ distribution in the reaction $e^-q \to e^-\gamma q$ for the SM background and the signal (for $f = f^{'} = 1$) with the inclusion of an excited electron with masses $m_\star = 200$ GeV, $m_\star = 400$ GeV, $m_\star = 800$ GeV and $m_\star = 1200$ GeV.

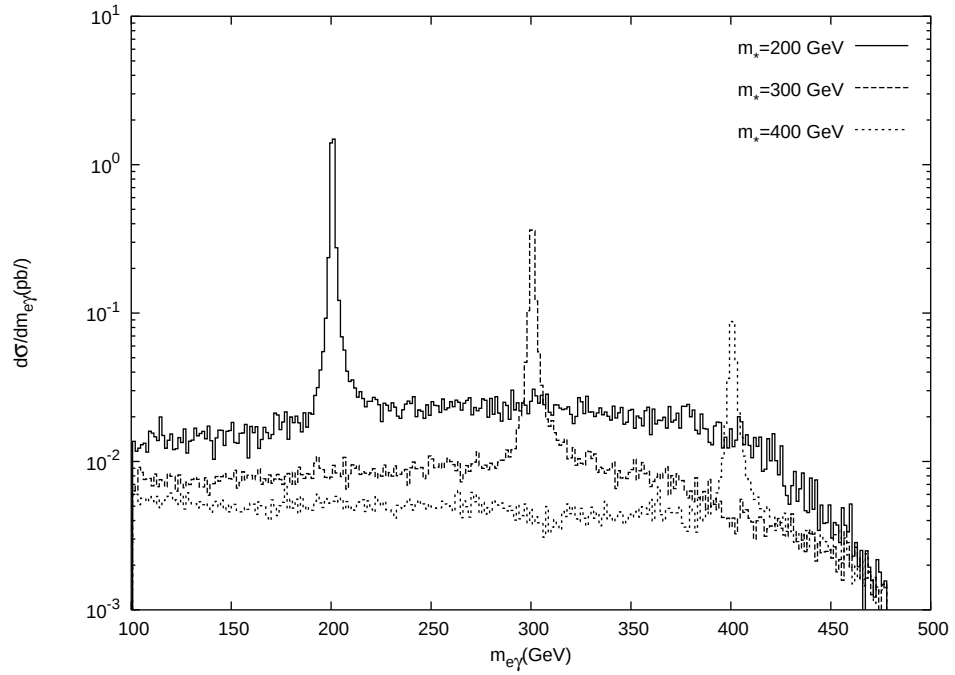


Figure 4: Invariant mass $m_{e\gamma}$ distribution of signal (the scale $\Lambda = m_*$ and the coupling parameters $f = f^{'} = 1$) and background at e^-e^+ collider.

Table I: The cross sections of the excited electron signal and relevant backgrounds after the cuts at e^-e^+collider with $\sqrt{s} = 0.5$ TeV and $L_{int} = 10^5 \text{fb}^{-1}$ assuming $\Lambda = m_\star$ and $f = f' = 1$.

$m^\star$(GeV)	σ_{S+B}(pb)	σ_B(pb)	SS
200	5.93×10^0	1.35×10^{-1}	4992.0
250	3.27×10^0	1.68×10^{-1}	2395.8
300	1.95×10^0	2.02×10^{-1}	1226.9
350	1.14×10^0	2.26×10^{-1}	606.9
400	6.49×10^{-1}	1.86×10^{-1}	185.4
475	3.17×10^{-1}	1.16×10^{-1}	81.3

In Table II, we present the signal and background cross sections in $e\gamma$ invariant mass bins satisfying the condition $|m_{e^-\gamma} - m_\star| < 25$ GeV for the mass range $m_\star = 200 - 1200$ GeV and $|m_{e^-\gamma} - m_\star| < 50$ GeV for $m_\star = 1200 - 2500$ GeV. For various coupling parameters $f(= f^{'})$, we show the mass dependence of the SS in Fig. 8. As can be seen from Table II LC⊗LHC can discover excited electron in $e^\star \to e\gamma$ decay mode for $f = f^{'} = 1$ up to the mass of 2300 GeV. This limit is larger than the corresponding one which can be reached at 500 GeV e^+e^- collider.

A common feature of the e^+e^- and ep collisions with respect to the single production of excited electron is the prominent role played by t-channel photon exchange mechanism which generates large production rates. This also leads to the strong limits on the compositeness scale in case of the negative search.

C. pp Collider

At the LHC, the single production of excited electrons takes place through the subprocesses $q\bar{q} \to Z/\gamma \to e^\pm e^{\mp\star} \to e^\pm e^\mp \gamma$ and $q\bar{q}^{'} \to W^\mp \to \nu e^{\mp\star} \to \nu e^\mp \gamma$ via the Drell-Yan mechanism. The diagrams related to these subprocesses are shown in Fig. 9. After the acceptance cuts the total SM background cross sections are obtained as $\sigma_B = 1.16$ pb for the process $pp \to e^+e^-\gamma X$ and $\sigma_B = 1.35$ pb for $pp \to \nu e^-\gamma X$.

Fig. 10 shows the invariant mass $m_{e\gamma}$ distributions in the reactions $pp \to e^+e^-\gamma X$ and $pp \to \nu e^-\gamma X$ for the SM background and the signal (for $f = f^{'} = 1$) with the inclusion of an excited electron with masses $m_\star = 200$ GeV, $m_\star = 400$ GeV, $m_\star = 800$ GeV and $m_\star = 1200$ GeV. In Table III, we present the signal and background cross sections

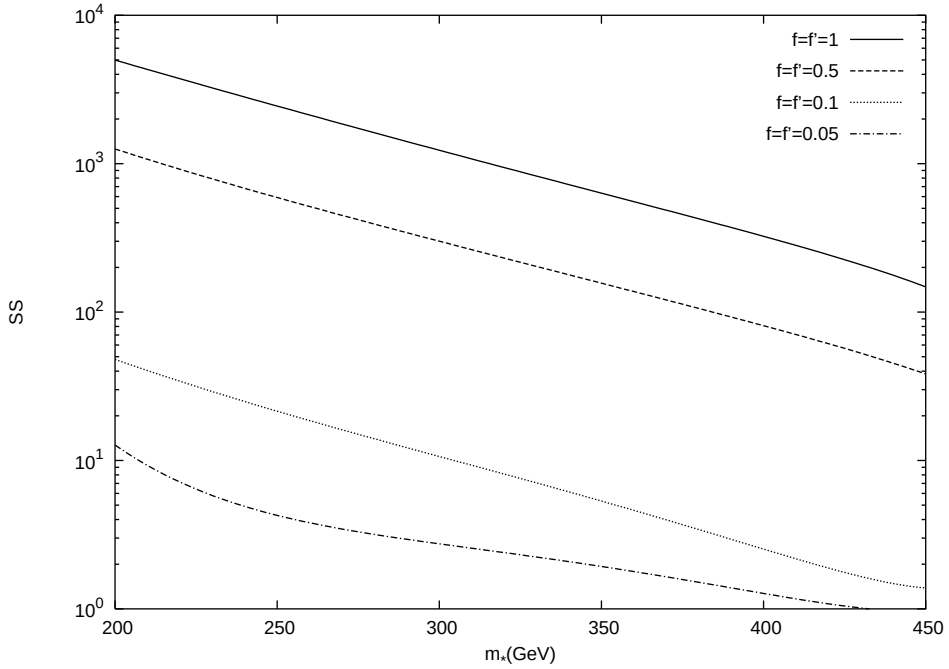


Figure 5: Statististical significance depending on the excited electron mass and different coupling parameters at the LC for the scale $\Lambda = m_*$.

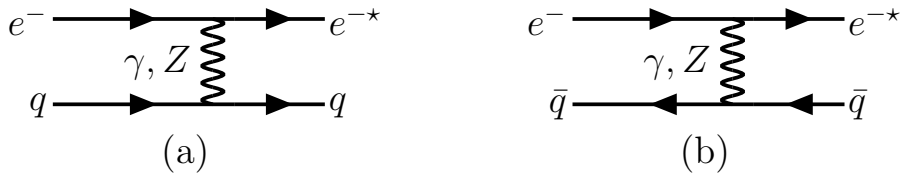


Figure 6: Single production of excited electrons at ep colliders through the subprocesses (a) $e^- q \to e^{-\star} q$ and (b) $e^- \overline{q} \to e^{-\star} \overline{q}$.

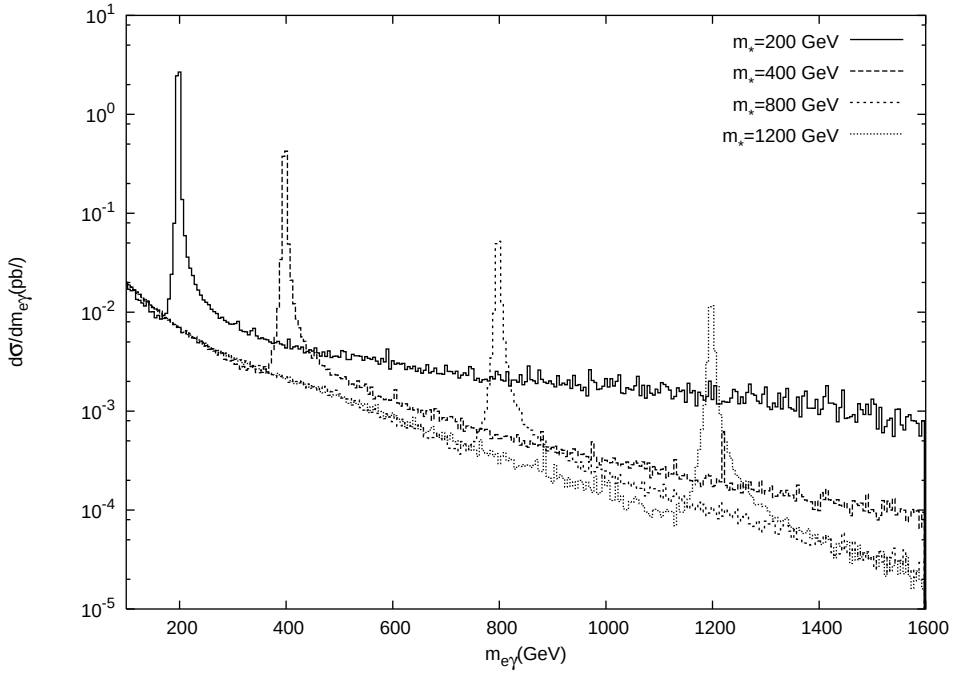


Figure 7: Invariant mass $m_{e\gamma}$ distribution of signal ($\Lambda = m_\star$ and $f = f^{'} = 1$) and background at $e^- p$ colliders.

Table II: The cross sections of the signal and relevant backgrounds at e^-p collider with $\sqrt{s} = 3.74$ TeV and $L_{int} = 100$ pb^{-1} assuming $\Lambda = m_\star$ and $f = f' = 1$.

Mass, GeV	$\Delta\sigma_{S+B}$(pb)	$\Delta\sigma_B$(pb)	SS
200	1.55×10^{1}	5.03×10^{-1}	2117.5
400	1.32×10^{0}	1.02×10^{-1}	696.5
600	6.68×10^{-1}	3.37×10^{-2}	345.4
800	2.78×10^{-1}	1.25×10^{-2}	237.1
1000	1.25×10^{-1}	4.44×10^{-3}	181.6
1200	6.23×10^{-2}	1.83×10^{-3}	141.3
1500	1.82×10^{-2}	1.17×10^{-3}	50.2
2000	5.63×10^{-3}	1.16×10^{-3}	13.1
2500	2.01×10^{-3}	1.16×10^{-3}	2.5

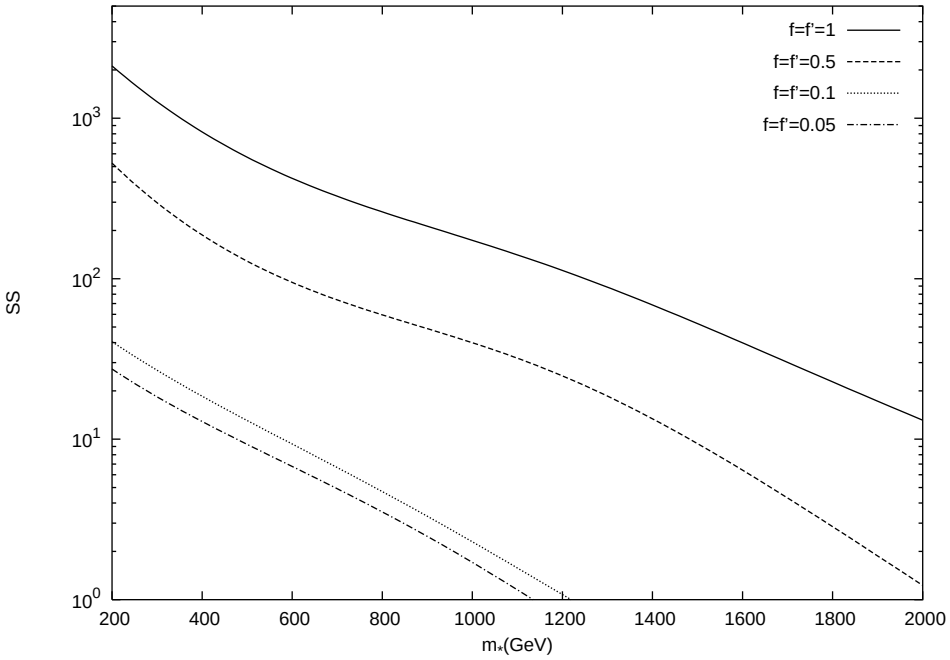


Figure 8: Statististical significance depending on the excited electron mass for different coupling parameters for the process$e^-p \to e^{-\star}q(\bar{q})X$ at the LC⊗LHC.

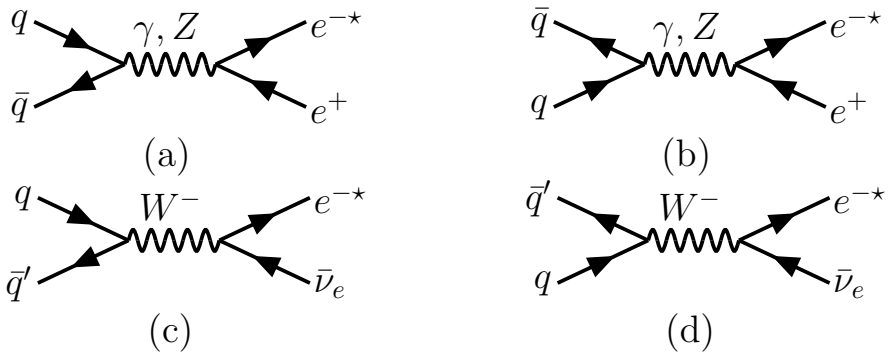
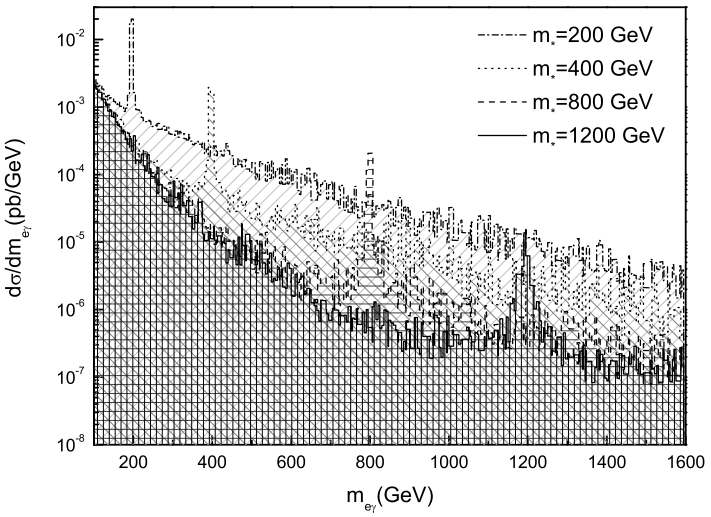
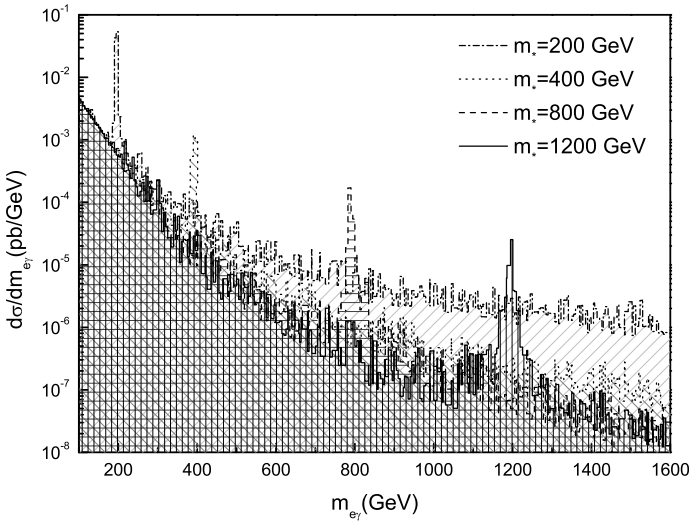


Figure 9: Excited electron production via the (a,b) photon and $Z-$boson exchange, and (c,d) W^-−boson in the $s-$channel diagrams at hadron colliders.



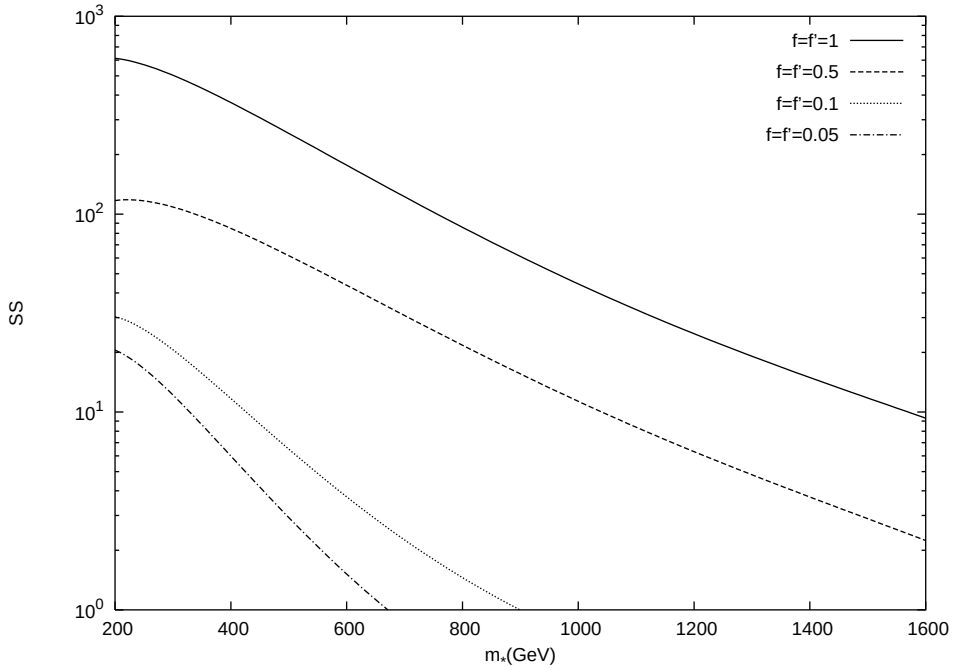
(a)



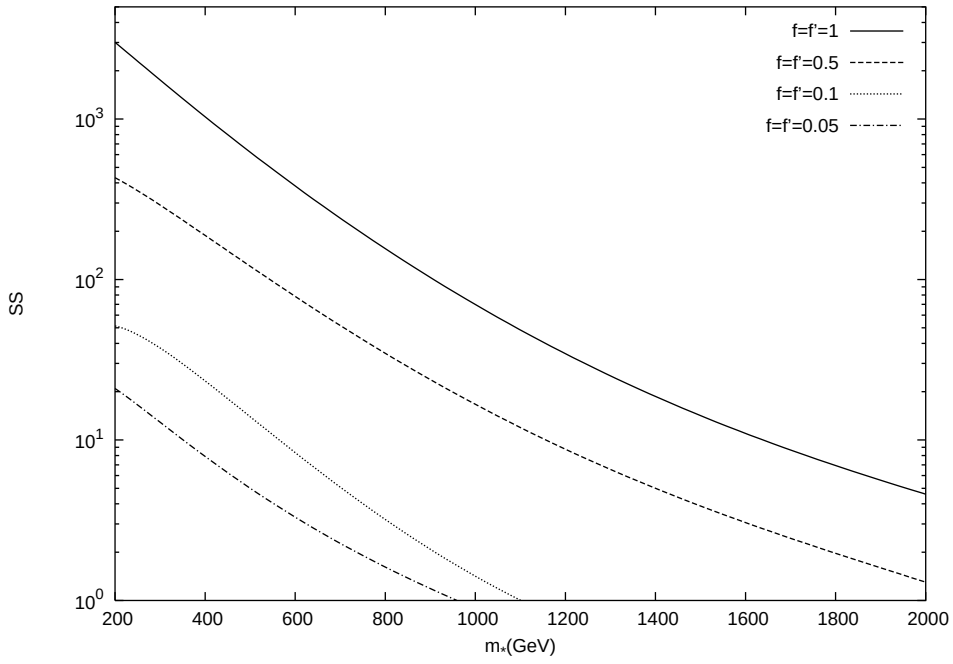
(b)

Figure 10: Invariant mass $m_{e\gamma}$ distribution of signal and background for the processes (a) $pp \to e^+e^-\gamma X$ and (b) $pp \to \nu e^-\gamma X$ at pp collider (LHC).

in $e\gamma$ invariant mass bins satisfying the condition $|m_{e^-\gamma} - m_\star| < 25$ GeV for excited electron mass $m_\star = 200 - 1200$ GeV and $|m_{e^-\gamma} - m_\star| < 50$ GeV for $m_\star = 1200 - 2500$ GeV. Statistical significance SS are shown in Fig. 11 (a) for $pp \to e^+e^-\gamma X$ and (b) for $pp \to \nu e^-\gamma X$ processes with different couplings $f(= f')$. One can conclude that the results obtained in this study turns out to be at least an order of magnitude more stringent than the present best limits coming from the HERA experiments. Moreover, the LHC will be able to extend considerably the range of excited electron masses that can be probed (up to about 2 TeV).



(a)



(b)

Figure 11: Statistical significance depending on the excited electron mass for process (a) $pp \to e^+e^-\gamma X$ and (b) $pp \to \nu e^-\gamma X$ with different couplings $f(= f')$ at the LHC.

Table III: The cross sections of the signal and relevant backgrounds at pp collider (LHC) with $\sqrt{s} = 14$ TeV and $L_{int} = 10^5 \mathrm{pb}^{-1}$. The statistical significance SS are given for the coupling $f = f' = 1$ and the scale $\Lambda = m^\star$.

Final states→	$e^-e^+\gamma$			$e^-\overline{\nu}\gamma$		
Mass, GeV	σ_{S+B}(pb)	σ_B(pb)	SS	σ_{S+B}(pb)	σ_B(pb)	SS
200	2.33×10^{-1}	1.29×10^{-2}	613.6	2.98×10^{-1}	9.79×10^{-4}	3003.8
400	2.24×10^{-2}	1.79×10^{-4}	524.4	2.52×10^{-2}	5.98×10^{-5}	1027.5
800	1.67×10^{-3}	8.01×10^{-5}	56.1	1.65×10^{-3}	2.28×10^{-5}	107.7
1200	3.13×10^{-4}	1.56×10^{-5}	23.8	2.91×10^{-4}	1.29×10^{-5}	24.4
1600	7.63×10^{-5}	5.75×10^{-6}	9.3	7.00×10^{-5}	5.81×10^{-6}	8.4
2000	2.26×10^{-5}	1.24×10^{-6}	6.1	1.97×10^{-5}	1.46×10^{-6}	4.8
2500	6.27×10^{-6}	7.35×10^{-7}	2.0	4.97×10^{-6}	6.14×10^{-7}	1.7

III. CONCLUSION

We give the realistic estimates for excited electron signal and the corresponding background at three-type of colliders with the availability of higher center of mass energies and higher luminosities. Since the cross section for the signal is proportional to $1/\Lambda^2$, various choices of the Λ, i.e. in this study we have choosen $\Lambda = m_\star$, will lead to the changes in the cross sections as $(m_\star/\Lambda)^2$. For $\Lambda = 1$ TeV, we need to multiply the signal cross sections by a factor $[m_\star(\mathrm{TeV})]^2$ at every mass values of excited electrons. This factor also extends the attainable mass limits for $m_\star > 1$ TeV. Our analysis show that for $f = f^{'} = 1$ LC can discover excited electron in $e^\star \to e\gamma$ decay mode up to the kinematical limit, while LC⊗LHC and LHC can reach much higher mass values, namely 2300 GeV and 1900 GeV, respectively. For $f = f^{'} = 0.05$ discover limits are: 240 GeV at LC, 650 GeV at LC⊗LHC and 450 GeV at LHC.

In our analysis, we assumed that the excited electron interact with the SM particles via the effective Lagrangian (1). In principle, excited electron may also couple to ordinary quarks and leptons via contact interactions which can enlarge discovery limits for pp colliders [9, 13] as well as for ep colliders. However, we restrict ourselves to the gauge interactions since the aim of this paper is to compare the potential of three types of colliders within the similar sets of cuts. Our results coincide with [10] where similar analysis was performed for the LC, and essentially coincide with [14] where different parton distribution functions, namely MRS (G) [15], have been used for the single production of excited electrons at the LHC. Finally, our analysis show that LC⊗LHC is more promising than the LHC and much more promising than the LC for the processes considered.

Acknowledgments

This work is partially supported by Turkish State Planning Committee under the Grants No 2002K120250 and 2003K120190.

[1] S. Sultansoy, Eur. Phys. J. C (2004) DOI 10.1140/epjcd/s2004-03-1716-2; hep-ex/0306034.
[2] H. Terazawa, Y. Chikashige and K. Akama, Phys. Rev. D **15**, 480 (1977); Y. Ne'eman, Phys. lett. B **82**, 69 (1979); H. Terazawa, M. Yasue, K. Akama and M. Hayashi, Phys. Lett. B **112**, 387 (1982).
[3] F. M. Renard, Il Nuovo Cimento A **77**, 1 (1983); E.J. Eichten, K.D. Lane and M.E. Peskin, Phys. Rev. D **50**, 811 (1983); A. De Rujula, L. Maiani and R. Petronzio, Phys. Lett. B **140**, 253 (1984); J. Kühn and P.M. Zerwas, Phys. Lett. B 147, 189 (1984).
[4] K. Hagiwara et al., Particle Data Group, Phys. Rev. D **66**, 010001 (2002).
[5] M. Acciarri et al., L3 Coll., Phys. Lett. B **502**, 37 (2001).
[6] C. Adloff et al., H1 Coll., Eur. Phys. J. C **17**, 567 (2000).
[7] P. Achard et al., L3 Coll., Phys. Lett. B **531**, 28 (2002).
[8] K. Hagiwara, S. Komamiya, and D. Zeppenfeld, Z. Phys. C **29**, 115 (1985).
[9] U. Baur, M. Spira and P.M. Zerwas, Phys. Rev. D **42**, 815 (1990).
[10] F. Boudjema, A. Djouadi and J.L. Kneur, Z. Phys. C **57**, 425 (1993); F. Boudjema, A. Djouadi, Phys. Lett. B **240**, 485 (1990).
[11] A. Pukhov *et al.*, hep-ph/9908288 (1999).
[12] H.L. Lai et al., CTEQ Collab., Phys. Rev. D **51**, 4763 (2000).

[13] O. Cakir *et al.*, Eur. Phys. J. C **30**, d01, 005 (2003).
[14] O.J.P. Eboli, S.M. Lietti and P. Mathews, Phys. Rev. D **65**, 075003 (2002).
[15] A. D. Martin, W.J. Stirling and R.G. Roberts, Phys. Lett. B **354**, 155 (1995).